Algerian Journal of Research and Technology
AJRTDZ@gmail.com
http://www.univ-usto.dz/AJRT/

ISSN : 2543-3954 *A.J.R.T Volume 2 (N° 1) (2018) 19-30*

Removal of Methylthioninium Chloride (MB) from Contaminated Water Media Using Activated Carbon Derived from Apricot Stones, a Low-cost Adsorbent

M. Abbas[a*], T. Aksil[b]

[a]*Laboratory of Soft Technologies and Biodiversity (LTDVPMBB), Faculty of Sciences, University M'hamed Bougara of Boumerdes, 35000 Algeria.*
[b] *University M'hamed Bougara of Boumerdes, Faculty of Sciences, Chemical Department 35000 Algeria.*

**Corresponding author. E-mail: moussaiap@gmail.com. Fax numbers: +213-024-91-11-16 Tel +213 52 40 84 19.*

Abstract. The preparation of activated carbon from apricot stone (ASAC) with H_3PO_4 and its ability to remove the (MB) used in the textile industry from aqueous solutions are reported in this study. The FTIR spectroscopy is used to get information on interactions between the adsorbent and MB. A series of contact time experiments were undertaken in stirred batch adsorber to assess the effect of the system variables. The results were discussed and showed that ASAC can be successfully used in the wastewater treatment. A comparison of two models on the overall adsorption rate showed that the kinetic of adsorption was better described by the pseudo-second order model. The adsorption isotherms of MB onto ASAC are determined and correlated with common isotherms equations. The smaller RMSE values obtained for the Langmuir and Elovich models indicate the better curves fitting, the monolayer adsorption capacity of MB is found to be 46.03 mg/g at 25 °C and 142.42 mg/g at 70 °C and pH 10. The thermodynamic parameters indicate spontaneous and endothermic nature of the adsorption process. The positive entropy ($\Delta S°$) shows that the randomness indecreases at the solid-solution interface during the MB adsorption onto ASAC, indicating that some structural exchange may occur among the active sites of the adsorbent and MB ions.

Keywords. Apricot stone, Chlorure de méthylthioninium, Kinetic, Isotherm, Adsorption, Thermodynamic.

INTRODUCTION

The effluents from the textile, leather, food processing, dyeing, cosmetics, paper and dyes manufacturing industries are important sources of pollution. Many dyes and their break down products may be toxic for living organisms particularly (MB) (Moussa et al., 2015). Therefore,

decolorizations of dyes are important aspects of the wastewater treatment before their discharge in the aquatic environment. It is difficult to remove the dyes from such effluents, because they are not readily degradable and are generally not removed from the sewage by conventional techniques. The electrochemical treatment, coagulation and flocculation, chemical oxidation, liquid-liquid extraction and adsorption were found to be effective for removing organic matter from aqueous solutions in terms of initial cost, simplicity of design, ease of operation and insensitivity to toxic substances (Kannan and Sundaram, 2001). The synthetic dyes are among the main contaminants in the aquatic medium accounting for about 20% of the total pollution. They cause several problems beginning by disturbing the eco-system: their presence in water, even at very low concentrations, is highly visible and undesirable; the coloration attenuate considerably the penetration of sunlight into water; retards the photosynthesis; inhibits the growth of aquatic biota and interferes with gas solubility in water bodies. In addition, the dyes in water gives rise to a chemical oxygen demand, biochemical oxygen demand and high-suspended solids. They are complicated organic compounds; they resist to the light, washing and microbial invasions and therefore cannot be decomposed easily (Lata et al., 2007). Direct discharge of dyes containing effluents may cause the formation of toxic carcinogenic breakdown products. The highest rates of toxicity were found amongst basic and diazo direct dyes (Bezaldez et al., 2008) . Activated carbon is the versatile adsorbent which has been used widely for the adsorption process, but remains relatively expensive. Consequently, many authors have studied the feasibility of low cost and abundantly available substances that are used for the synthesis of activated carbon. Therefore, , this has prompted a growing research interest in the production of activated carbons from renewable and cheaper precursors which are mainly industrial and agricultural by-products, for the wastewater treatment. However, the activated carbons available in the commerce are relatively expensive and their production and regeneration may constitute limiting factors. Hence, many researchers have focused on the search on new low-cost precursors issued from agricultural wastes such as rubber seed coat, pecan shells, jute fiber, Indian rosewood sawdust, olive stones, pinewood, sawdust, coir pith, rice husk, bamboo, rattan sawdust, oil palm fiber and apricot stone.
(Wang et al., 2008a ; Rengaraj et al., 2002; Senthil kumaar et al., 2005 ; El-Sheikh et al., 2004 ; Malik, 2004 ; Guo et ., 2005 ; Hameed et al., 2007 ; Mousa et al., 2014 ; Mouni et al., 2001 ; Mousa et al., 2015 ; Ozer et Dursum, 2007 ; FAO, 2009 ; Giles et al., 1960). The remarkable adsorption capacity of activated carbons is due to their well-developed porous structure and pore size distribution, as well as the surface functional groups. ASAC has exceptional mechanical properties, unique electrical property, highly chemical stability and large specific surface area, So, ASAC has attracted a great interest as adsorbent type and offers an attractive option for the removal of both organic and inorganic contaminates (Gerent et al., 2007; Crini et al., 2007). In the present work, ASAC is selected as an adsorbent to remove methylene blue from aqueous solution. (MB) is the most commonly used substance for dyeing cotton, wood and silk. Although, MB is not strongly hazardous, it is however responsible of several harmful effects where acute exposure to MB will cause increased heart rate, nausea, vomiting, shock, cyanosis, jaundice, and quadriplegia and tissue necrosis in humans (Bulut and Baysal, 2006). The main objective of this research was to evaluate the adsorption aptitude of ASAC for the removal of (MB), a model compound for basic dyes. The effects of pH, contact time, initial dye concentration, stirring speed, adsorbent dosage and temperature on the adsorption capacity were investigated. Moreover, the kinetic and equilibrium models were used to fit the experimental data and the thermodynamic parameters were determined. Agricultural by-products exist in large amounts and about 20.000 tonnes of apricot stones are produced annually in Algeria (Allen et al., 2004) (Table 1). Over the past, these by-products were used as fuel in rural areas but currently the preparation of activated carbon is considerably encouraged. Apricot stone is a cheap precursor for the activated carbon source. Therefore, it is important to evaluate its

performance as adsorbent. In previous studies, we have developed adsorbent materials with different properties, to achieve selective applications depending on the molecules to be separated.

Table 1. The state of apricot culture in 2010.

Year	Production x (1000 tonnes)
2000	56354
2001	67724
2002	73733
2003	106469
2004	87991
2005	145097
2006	167017
2007	116438
2008	172409
2009	202806
2010	239700

EXPERIMENTAL

Materials and methods

Analytical grade reagents are used in all experiments. Basic dye, MB (99 %) is purchased from Merck Company. The properties of MB are listed in table 2. Activated carbon was prepared by a conventional method: carbonization and chemical activation with phosphoric acid as follows: Apricot stones obtained from Boumerdes region (50 km east Algiers), are air-dried, crushed and screened to obtain two fractions with geometrical mean sizes of 63 and 2.5 mm. 100 g of the selected fraction are impregnated with concentrated H_3PO_4 (85%) and dried in air. Then, it is activated in a muffle furnace oven at 250 °C (4 h). The carbonized material is washed with distilled water to remove the free acid until the pH reaches 6.8 and dried at 105 °C. The clean biomass is mechanically ground and sifted to get powders of different particle sizes : < 63 µm to 2 mm.

Table 2. Chemical and physical properties.

Chemical properties		
Brute	Formula	$\underline{H_{18}ClN_3S}$
Molecular weight	(319.852 ± 0.022) g/mol	
Composition (%)	C : 60.08 , N :13.00, Cl: 11.08 H : 5.67, S : 10.03	
Wave number (λ_{max})	662 nm	
Name	Methylene Blue (MB) (C.I. Basic Blue 9)	
Physical properties		
Melting temperature	180 °C	
Solubility in water	50 g/L at T = 20 °C	
Solubility in alcohol	10 g/L at T = 20 °C	

Activated carbon characterization

Chemical and physical analysis of the prepared ASAC

The prepared activated carbon was characterized by selected physical properties (bulk density and surface area), chemical and adsorption properties (point of zero charge: pH_{pzc}). The elemental analysis was performed by using an elemental analyzer LECO-CHNS 932. The specific surface area of the activated carbon was achieved by using the BET-technique, as a sorption phenomenon of nitrogen gas on the adsorbent surface, at 77 K. The measurements were made using a Pore Size Micrometric-9320, USA equipment. The ash content Ash (%) of the activated carbon was determined by using a muffle furnace over 3 h at 450 °C. The conductivity measurements were carried out with a conductimeter type Erwika. The pH_{pzc} of the ASAC was determined by using potassium nitrate. 20 mL of a KNO_3 solution (0.01 M) were placed in different closed conical flasks. The pH of each solution in flask has been adjusted between 2 and 14 by adding solutions of HCl (0.1 M) or NaOH (0.1 M). Then, 0.1 g of ASAC was added and the final pH was measured after 24 h under agitation at room temperature. The pH_{pzc} is the point where the curve of final pH versus initial pH crosses the line: final pH = initial pH (Ozcan et al., 2006).

Structural and morphological

The infrared analysis of the prepared ASAC was performed by using an IR spectrophometer of FT Bomen-Michelson type. The IR spectrum was obtained by grinding 2 mg of the ASAC sample with 98 mg of spectroscopic KBr. The mixture was pressed at elevated pressure into a small disc of 1 cm in diameter and 2 mm in thickness. The X-ray diffraction patterns of the native apricot stone (NAS) and prepared ASAC were obtained with a Philips X-ray diffractometer (PW 1890 model).

Batch mode adsorption studies

The effects of the experimental parameters such as adsorbent dosage (1-10 g/L), agitation speed (100-1200 rpm), the initial MB concentration (2-14 mg/L), pH (2-14) and temperature (293-343 K) on the adsorptive removal of MB ions are studied in a batch mode of operation for a variable specific period of contact time (0-60 min). The MB solutions are prepared by dissolving the accurate amount of MB (99 %) in distilled water, used as a stock solution and diluted to the required initial concentration; pH is adjusted with HCl (0.1 mol/L) or NaOH (0.1 mol/L). For the kinetic studies, desired quantities of ASAC is contacted with 10 mL of MB solutions in Erlenmeyer flasks. Then, the flasks are placed on a rotary shaker at 300 rpm and the samples are taken at regular time intervals and centrifuged at 3000 rpm for 10 min. The MB content in the supernatant was analyzed on a Perkin Elmer UV-visible spectrophotometer model 550S at (λ_{max} = 662 nm). The amount of MB ions adsorbed by activated carbon q_t (mg/g) is calculated by using the following equation (1) :

$$q_t = \frac{(C_0 - C_e)\cdot V}{m} \quad (1)$$

Where C_o is the initial MB concentration and C_t the MB concentrations (mg/L) at any time, V the volume of solution (L) and m the mass of the activated carbon (g). Due to the inherent bias resulting from linearization of the isotherm models, the non-linear regression Root Mean Square Error (RMSE) equation (2), the Sun of Error Squares (SSE) equation (3) and Chi-Squares (X^2) equation (4) test are employed as criterion for the quality of fitting (Crini et al., 2007).

$$\mathrm{RMSE} = \sqrt{\frac{1}{N-2}\cdot\sum_1^N (q_{e,exp} - q_{e,cal})^2} \quad (2)$$

$$\mathrm{SSE} = \frac{1}{N}\sum_{n=1}^{\infty} \left(qe_{cal} - qe_{exp}\right)^2 \quad (3)$$

$$X^2 = \sum_1^N \frac{(q_{e,exp} - q_{e,cal})^2}{q_{e,cal}} \quad (4)$$

Where, $q_{e(exp)}$ ($mg.g^{-1}$) is the experimental value of uptake, $q_{e(cal)}$ the calculated value of uptake using a model ($mg.g^{-1}$) and N the number of observations in the experiment (the number of data points). The smaller RMSE value indicates the better curve fitting (Oczen et al., 2006).

RESULTS AND DISCUSSION

Characterization of the prepared ASAC

The physical and chemical properties of ASAC and the elementary analysis are summarized in table 3.

Table 3. Chemical and physical properties of Basic dye, Methylene Blue.

Elemental analysis of ASAC (%)	C : 48.45 H : 6.03 N : 0.44 O : 45.08
pHzpc	7.05 ± 0.10
Surface area (m^2/g)	88.05 ± 1.03
Average pore diameter (Å)	176.32 ± 0.25
Average pore volume (mL/g)	0.2641± 0.003
Conductivity (µS/cm)	112.0 ± 2
Humidity (%)	1.48 ± 0.16
The rate of ash (%)	1.68 ± 0.02
The percentage of organic matter (%)	98.32 ± 0.11

Structural characterization by infrared spectroscopy

The spectra of the adsorbent display a number of absorption peaks, indicating that many functional groups are present in the adsorbent. Peaks are observed at 3436, 2929, 1732, 1599 and 1508 cm^{-1}. These results clearly indicate that the functional groups including carboxylic and hydroxyl groups contribute to the adsorption acid dye ions.

Effect of analytical parameters

In the first stage of batch adsorption experiments on ASAC, the effect of particle sizes on the acid dye adsorption by ASAC is examined. Significant variations in the uptake capacity and removal efficiency were observed at different particles sizes, indicating that the best performance is obtained with lower particle sizes (315-800 µm). In general, smaller particles provide large surface area, resulting in high acid dye uptake capacity and removal efficiency. The particle size range (315-800 µm) is subsequently used in all adsorption experiments.

The pH of the BM solution plays an important role in the adsorption process**.** It is evident that the percentage of acid dye removal increases consistently with decreasing pH. The effect of pH on the adsorption by ASAC can be explained on the basis of the point of zero charge ($pH_{zpc,}$), for which the adsorbent surface is neutral. The surface charge of the adsorbent is positive when the medium pH is under pH_{zpc} and negative for higher pH pH_{zpc} of ASAC is 7.05 and the surface charge of ASAC is negative at higher pH. As the pH decreases, the number of positively charged sites increases and favours the adsorption of MB ions by electrostatic attractions. Similar experimental details have been reported (Crini et al., 2007).

The effect of the stirring speed on the MB dye adsorption capacity onto the prepared ASAC. The maximum uptake was obtained for a speed of 300 rpm. Such moderate speed gives a good homogeneity for the mixture suspension.

The adsorption capacity of MB increases with time and attains a maximum after 40 min and thereafter and reaches a constant value, indicating that no more MB ions are further removed from the solution. The equilibrium time is found to be 45 min. The initial concentration of acid dye from 2 to 14 mg/L, leads to increased adsorbed amount from 1.9 to 7. 1 mg/g. This may be attributed to an increase of the driving force due to the concentrations gradient with increasing

the initial dye concentration in order to overcome the mass transfer resistance of MB ions between the aqueous and solid phases.
For the first stage of batch adsorption experiments on ASAC, the effect of adsorbent dosage on the acid dye adsorption is examined. Significant variations in the uptake capacity and removal efficiency observed at different adsorbent dosages (1-10 g/L) indicate that the best performance is obtained with a dosage of 1 g/L. This result was expected because the removal efficiency generally increases by the fact that more mass available, more the contact surface offered to the adsorption. Moreover, higher dose of adsorbent in the solution, greater availability of exchangeable sites for the ions, i.e. more active sites are available for binding of MB ions.

Adsorption Isotherms
The shape of the isotherms is the first experimental tool to diagnose the nature of a specific adsorption phenomenon. The isotherms have been classified according to Giles et al., (1960) in four main groups: L, S, H, and C, and the isotherm of ASAC at different temperatures (25 ^{o}C and 70 ^{o}C) displays both L and S type curves (Fig. 1a,1b) (Ho and Mc Kay, 2000). The initial part of the L curve indicates a small interaction between the basic dye and the carrier at low concentrations. However, as the concentration in the liquid phase increases, the adsorption occurs more readily. This behaviour is due to a synergistic effect, with the adsorbed molecules facilitating the adsorption of additional molecules as a result of attractive interaction adsorbate-adsorbate. Equilibrium isotherm equations are used to describe the experimental adsorption data. The equation parameters and the underlying thermodynamic assumptions of these equilibrium models often provide some insights into both the sorption mechanism and the surface properties and affinity of the adsorbent.

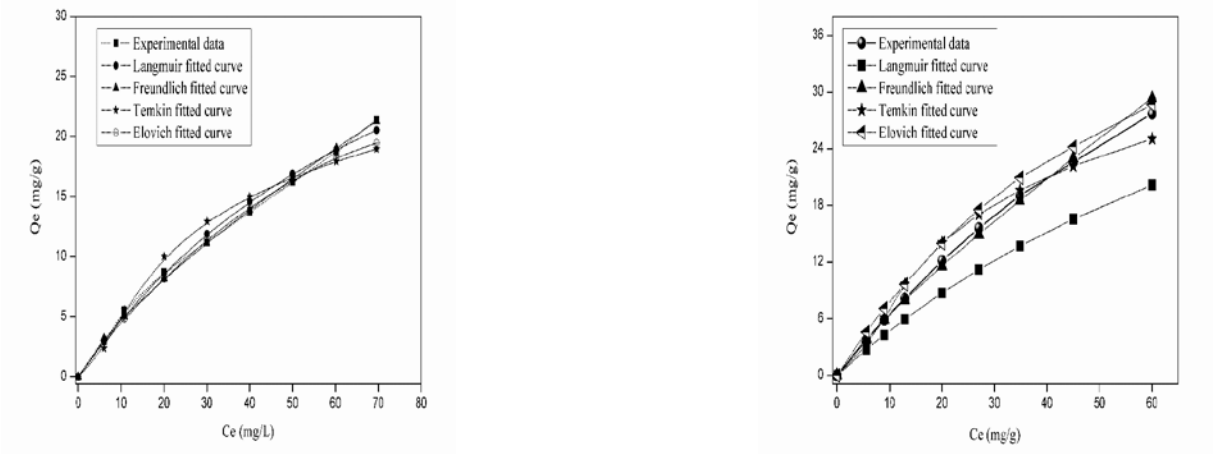

a. at temperature 70 °C. b. at temperature 25 °C.
Fig. 1. Adsorption isotherm of MB by ASAC.

- The Langmuir equation it is represented by the linear form (Weber and Chackravorti, 1974):

$$\frac{1}{q_e} = \frac{1}{q_{max}} \cdot \frac{1}{q_{max} \ .K_L.Ce} \quad (4)$$

Where C_e is the equilibrium concentration (mg7L), q_{max} the monolayer adsorption capacity (mg/g) and K_L the constant related to the free adsorption energy (Langmuir constant, L/mg). Therefore a plot of $1/C_e$ versus $1/q_e$ (Fig.2) and $1/q_e$ versus $1/C_e$ (Fig.3) enables the determination of the constant K_L and Q_{max}.

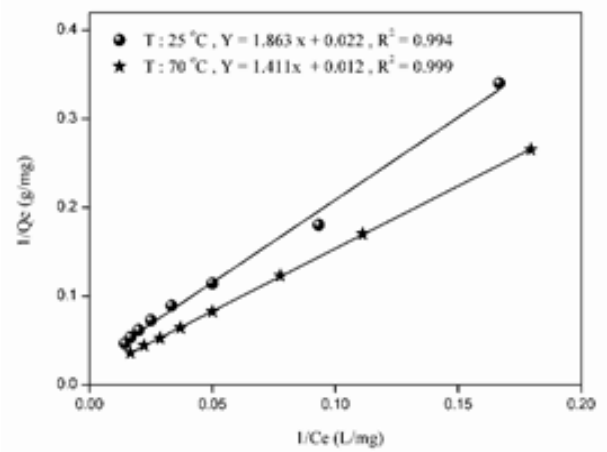

Fig.2. The Langmuir isotherms (type I) for the adsorption of MB ions onto ASAC.

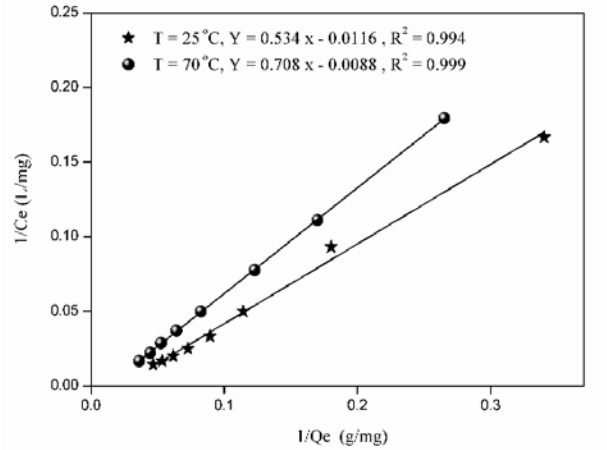

Fig.3. The Langmuir isotherms (type V) for the adsorption of MB ions onto ASAC.

The RMSE values obtained at 25 °C for the models indicate a better fitting. The essential features of the Langmuir isotherm R_L indicates the type of isotherm: irreversible ($R_L = 0$), favourable ($0 < R_L < 1$), linear ($R_L = 1$) or unfavourable ($R_L > 1$). In this study, the R_L values are less than 1, thus confirming that the adsorption process is favoured in both cases as well as the applicability of Langmuir isotherm (Kin et al., 2012)**.**

- The Freundlich isotherm can be applied to nonideal adsorption on heterogeneous surfaces as well as multilayer sorption; is expressed by the following equations (5) (Kin et al., 2012)**.**

$$\mathrm{Ln}\, q_e = \mathrm{Ln}\, K_F + \frac{1}{n} \cdot \mathrm{L\,n}\, Ce \quad (5)$$

The constant K_F indicates the adsorption capacity of the adsorbent (L/g) and n is an empirical constant related to the magnitude of the adsorption driving force. Therefore, a plot of Lnq_e versus LnC_e (Fig.4) enables the determination of the constant K_F and exponent n.

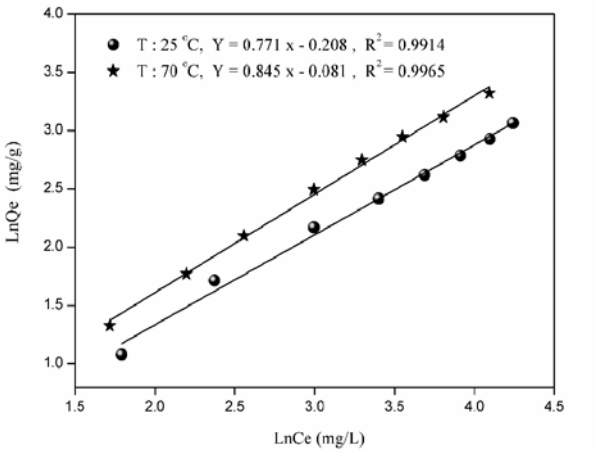

Fig.4. The Freundlich isotherms for the adsorption of MB ions onto ASAC.

- The Temkin isotherm describes the behavior of adsorption systems on heterogeneous surfaces, and it has generally been applied in the following form equation (6) (Ghaedj et al., 2013).

$$Qe = \frac{RT}{b} LnA + \frac{RT}{b} LnCe = BLnA + BLn\ Ce \quad (6)$$

The adsorption data can be analyzed according to equation (6). Therefore, a plot of qe versus LnCe enables to determine the constants A and B.

- The Elovich isotherm is based on the principle of the kinetic assumes that the number of adsorption sites increases exponentially with the adsorption, which implies a multilayer adsorption described by equation (7) (Benguella and Yacouta Nour, 2009).

$$Ln\ \frac{q_e}{C_e} = Ln\ q_m\ .\ K_E\ \frac{q_e}{q_m} \quad (7)$$

Where K_E (L/mg) is the Elovich constant at equilibrium, q_m (mg/g) the maximum adsorption capacity, q_e (mg/g) the adsorption capacity at equilibrium and C_e (g/L) the concentration of the adsorbate at equilibrium. If the adsorption is described by the equation of Elovich, the equilibrium constant and the maximum capacity can be calculated from the plot of Ln (q_e/C_e) versus q_e.

The theoretical parameters of adsorption isotherms along with the regression coefficients, RMSE, SSE and X^2 are listed in table 4. The Freundlich isotherm model exhibits the higher RMSE, X^2 and SSE values.

Adsorption kinetics

The kinetic study is important for the adsorption process, it describes the uptake rate of adsorbate and controls the residual time of the whole adsorption process. Two kinetic models namely the pseudo first order and pseudo second-order are selected in this study to describe the adsorption.

- The pseudo first order equation is given in equation (8) (Jerald, 2012):

$$\log(q_e - q_t) = \log q_e - \frac{K_1}{2.303} \cdot t \quad (8)$$

- The pseudo second order model is expressed by the equation (9) (Faust et al., 1959; Vousdria et al., 2002):

$$\frac{t}{q_t} = \frac{1}{K_2 \cdot q_e^2} + \frac{1}{q_e} \cdot t \quad (9)$$

Where q_t (mg/g) is the amount of metal adsorbed on the adsorbent at various times t (min), K_1 the rate constant of the pseudo-first order kinetic (min^{-1}), K_2 the rate constant of the pseudo-second order kinetic (g/mg.min). For the pseudo-first order kinetic, the experimental data deviate greatly from linearity. This was evidenced by the low values of q_e and determination coefficients. Therefore, the pseudo-first order model is inapplicable to this system. The

determination coefficient and $q_{e,cal}$ of the pseudo-second order kinetic model are in good agreement with the experimental results (Table 5).

Table 4. Sorption isotherm coefficients of Langmuir, Freundlich, Temkin and Elovich models.

Temperature	T = 25 °C		T = 70 °C	
Models	Parameters		Parameters	
Langmuir (I)	Q_{max} : 45.45 mg/g		Q_{max} : 83.33 mg/g	
	K_L : 0.0118 g/mg		K_L : 0.0085 g/mg	
1/Qe = f (1/Ce)	R^2	0.994	R^2	0.999
	RMSE	0.125	RMSE	0.889
	SSE	0.156	SSE	0.790
	X^2	0.020	X^2	0.860
Langmuir (V)	Q_{max} : 46.03 mg/g		Q_{max} : 88.5 mg/g	
	K_L : 0.0116 g/mg		K_L : 0.0088 g/mg	
1/Ce = f (1/ce)	R^2	0.994	R^2	0.999
	RMSE	0.125	RMSE	0.889
	SSE	0.156	SSE	0.790
	X^2	0.020	X^2	0.860
Freundlich	K_F : 0.812 mg/g		K_F : 0.922 mg/g	
	1/n : 0.77		1/n : 0.845	
LnQe = f(LnCe)	R^2	0.991	R^2	0.999
	RMSE	0.070	RMSE	0.496
	SSE	0.005	SSE	0.246
	X^2	0.021	X^2	0.028
Elovich	Q_{max} : 33.30 mg/g		Q_{max} : 142.8 mg/g	
	K_L : 0.016 g/mg		K_L : 0.0088 g/mg	
Ln(Qe/Ce) = f (qe)	R^2	0.584	R^2	0.89
	RMSE	0.213	RMSE	0.227
	SSE	0.046	SSE	0.051
	X^2	0.072	X^2	0.073
Temkin	K_E : 0.202 L/mg		K_E : 0.2028 L/mg	
	β_T : 7.18		β_T : 10.028	
Qe = f(LnCe)	ΔQ : 15.538 kJ/mol		ΔQ : 25.167 kJ/mol	
	β_T : $RTQ_m/\Delta Q$		β_T : $RTQ_m/\Delta Q$	
	R^2	0.937	R^2	0.948
	RMSE	0.294	RMSE	0.357
	SSE	0.087	SSE	0.127
	X^2	0.591	X^2	1.835

Intraparticle diffusion study

An empirically found functional relationship common to most adsorption process is that varies almost proportionally with $t^{1/2}$, the Weber-Morris plot (q_t versus $t^{1/2}$), rather than with the constant time t equation (10) (Weber and Chackravorti, 1974).

$q_t = K_{in} t^{½} + C$ (10)

Where K_{in} is the intraparticle diffusion rate constant. Values of intercept C gives an idea about the thickness of boundary layer (Suteu and Bilba, 2005). This is attributed to the instantaneous utilization of the most readily available adsorbing sites on the adsorbent surface.

The values of K_{in} and C obtained from the slope and intercept of linear plots and the constant of the modified Freundlich model and Elovich model are listed in table 5.

Table 5. Kinetic parameters for adsorption of MB ions onto ASAC.

	2^{ieme} Ordre					Pseudo 1 Ordre			
C_o (mg/L)	Q_{ex} (mg/g)	Q_{cal} (mg/g)	R^2	ΔQ/Q (%)	K_2 (g/mg.mn)	Q_{cal} (mg/g)	R^2	ΔQ/Q (%)	K_1 (mn^{-1})
2	1.01	1.22	0.994	17.07	0.0714	1.002	0.977	0.79	1.22
5	3.81	3.95	0.999	3.5	0.1425	2.333	0.974	38.76	3.95
10	4.93	5.15	0.999	4.3	0.0856	3.029	0.954	38.40	5.15
14	6.93	7.15	0.996	6.8	0.3191	6.292	0.953	9.235	7.15
		Elovich			Diffusion				
C_o (mg/L)	R^2	β (g/mg)	α (mg/g.mn)		C_o (mg/L)	K_{in} ($mg/g.mn^{1/2}$)	R^2	C ($mn^{1/2}$)	D Cm^2/s
2	0.983	4.274	0.298		2	0.0825	0.86	0.4066	
5	0.931	1.808	14.03		5	0.0231	0.90	3.6400	0.5210^{-7}
10	0.981	1.488	22.99		10	0.0918	0.86	4.2500	
14	0.979	0.88	9.814		14	0.2717	0.77	4.9600	

The adsorption mechanisms and the kinetics can be described according to several models, which can predict the breakthrough curves at different times and accuracies. However, there are not clear criteria to estimate which is the most convenient for a given case, and a lot of concerns must be considered: the mass transfer resistances involved, relation type between the adsorbed amount and the diffusion coefficients, definitive equilibrium equation and description level and mathematical complexity of the model. It is well known that a well carried out batch experiment should give valuable data to estimate the diffusion coefficients. Usually, in the real conditions, the mass transport resistance inside the solid is very much higher than through the external fluid film on the solid particles.

Effect of temperature

The adsorption capacity of ASAC increase from 0.5 to 7.33 mg/g with increasing temperature (293 to 343 K), indicating that the adsorption is disfavored at high temperature. The thermodynamic parameters i.e. the free energy (ΔG^o), enthalpy (ΔH^o) and entropy (ΔS) are determined from the following equations (11) and (12) (Stephansen and Sheldo, 1996; Zou et al., 2013)

$\Delta G^o = - RT \, LnK$ (11)

$\Delta G^o = \Delta H^o - T\Delta S^o$ (12)

The thermodynamic equilibrium constant K for the sorption was determined by Khan and Singh by plotting q_e/C_e versus C_e and extrapolating to zero q_e (Ghaedj et al., 2013).

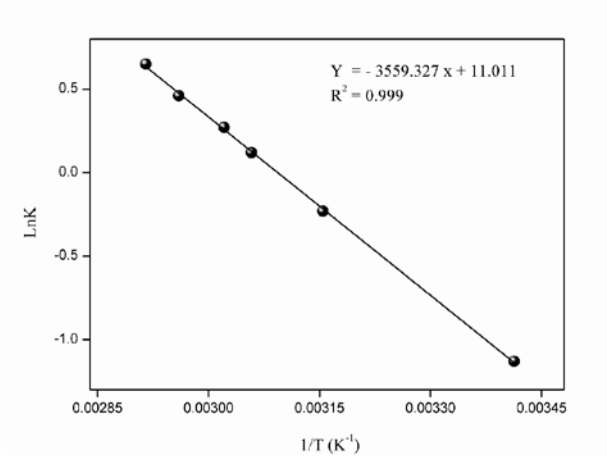

Fig.5. Thermodynamic parameters for the adsorption of MB ions onto ASAC.

The ΔH^o and ΔS^o values obtained from the slope and intercept of Van't Hoff plots of LnK versus 1/T (Fig.5) and the ΔG^o values at various temperatures are **summarized in table 6.**

Table 6. Thermodynamic parameters for the MB adsorption on ASAC.

T (K)	1/T (K^{-1})	K	LnK	ΔG (KJ/mol)	ΔH (KJ/mol)	ΔS (J/mol. K)
293	3.41296 10^{-3}	0.336216	-1.09	+ 2.70025		
317	3.15455 10^{-3}	0.794534	-0.23	+ 0.55615		
327	3.0581 10^{-3}	1.080042	0.077	- 0. 33722	28.87613	89.33749
331	3.0210 10^{-3}	1.309964	0.27	- 0.69394		
337	3.010 10^{-3}	1.580739	0.46	-1.23060		
343	2.9673 10^{-3}	1.915541	0.65	- 1.76666		

CONCLUSION

This study has shown that the activated carbon prepared from apricot stone can be employed as effective adsorbent for the removal of MB from aqueous solution. The Elovich and Langmuir isotherms model provided a better fit of the equilibrium adsorption data one. They gave a maximum adsorption capacity of 46.03 mg/gat 25 ºC which increased to 142.8 mg/g at 70 ºC at pH 10. The pseudo-second order model proved the best description of the kinetic data. The negative value of ΔG^o and positive value of ΔH^o indicate that the adsorption of MB onto ASAC is spontaneous and endothermic over the studied range of temperatures. The positive value of ΔS^o states clearly that the randomness increases at the solid-solution interface during the MB adsorption onto ASAC, indicating that some structural exchange may occur among the active sites of the adsorbent and the ions. The adsorption of MB ions by ASAC follows a pseudo-second order kinetic model, which relies on the assumption that chemisorptions may be the rate-limiting step. In chemisorption, the MB ions are attached to the adsorbent surface by forming a chemical bond and tend to find sites that maximize their coordination number with the surface. The kinetics and thermodynamic data can be further explored for the design of an adsorber for industrial effluents treatment.Acetic acid has been found effective for the regeneration of adsorbent than other solvents. It was noted during the experiments in the laboratory in batch mode that the adsorbent regenerated after several washings showed a decrease of the adsorption capacity (30 %) can be used again efficiently for subsequent use.This study in tiny batch gave rise to encouraging results, and we wish to achieve the adsorption tests in column mode under the conditions applicable to the treatment of industrial effluents and the

present investigation showed that ASAC is a potentially useful adsorbent for the metals, acid and basic dyes.

REFERENCES

Allen S.J., McKay G., Porter J.F. 2004. J. Colloid Interface Sci. 280, 222-333.
Benguella B., Yacouta Nour A. 2009. Compte Rendu de Chimie. 1-10.
Bezaldez E.E., Robaina N.F., Cassella R.J. 2008. J. Hazard. Mater. 159, 580 -586.
Bulut Y., Baysal Z. 2006. J of Envi Management. 2, 107-113.
Crini C., Peindy H.N., Gimbert F. 2007. Separ. Purif Technol. 53, 97-110.
El-Sheikh A.H., Newman A.P., Al-Daffaee H.K., Phull S., Cresswell N. 2004. J. Anal. Appl. Pyrolysis.71, 151–164.
FAO Annuaire de la production . 2009. Ed FAO Rome.
Faust G.T., Hathaway J.C., Millot G.A. 1959. Am. Miner. 44, 342-370.
Gerent C., Lee V.K.C., Le clorrek P., McKay G. 2007. Crit. Rev Environ. Sci. Technolol. 37, 41-121.
Ghaedj M., Karimi F., Barrazzch B., Saraei R., Danichfar A. 2013. J. Ind. Eng. Chem. 19 (3), 756.
Giles C.H., Mac Ewan T.H., Nakhwa S.N., Smith D. 1960. J. Chem. Soc. 10, 3973-3993.
Guo Y., Zhao J., Zhang H., Yang S., Qi J., Wang Z., Xu H.2005. Dyes Pigments. 66, 123–128.
Hameed B.H., Ahmad A.L., Latiff K.N.A. 2007. Dyes Pigments. 75, 143–149.
Ho Y.S., Mc Kay G. 2000. Water Res. 34 (3), 735-742.
Jerald M. 2012. Journal of Applied Biology and Pharmaceutical Technology. 3, 27-3.
Kannan N., Sundaram M.M. 2001. Dyes and Pigments. 51, 25-40.
Kin T.Y., Park S.S., Cho S.Y. 2012. J. Ind. Eng. Chem. 18(3), 1751.
Lata H., Gard V.K., Gupta R.K. 2007. Dyes Pigments. 653-658.
Lagergren S. 1998. K. Sven.Ventensskapsakad. Handlingar Band. 24, 1-39.
Malik P.K. 2004. J. Hazard. Mater. B113, 81–88.
Mouni L., Merabet D., Bouzaza A., Belkhiri L. 2001. Desalination. 276 (1-3), 148-153.
Moussa A., Kaddour S., Trari M. 2014. J . Ind. and Eng. Chem. 20, 745-751.
Moussa A., Abdelhamid C., Samia K., Tounsia A., Mohamed T.. 2015. J Environ Anal Toxicol. 5, 264.
Moussa A., Abdelhamid C., Kaddour S., Aksil T. 2015. Desalination and water treatment. 1-12.
Oladoja N.A., Aboluwoye C.O., Oladimeji Y.B. 2008. J. Eng Env Scien. 32, 303-312.
Ozcan A., Oncu E.M., Ozcan A.S. 2006. Physico-Chem. Eng, Aspects. 277, 90-97.
Ozer A., Dursun G. 2007. J .Hazard. 146, 262-269.
Rengaraj S., Moona S.H., Sivabalan R., Arabindoo B., Murugesan V. 2002. J. Hazard. Mater. B89, 185–196.
Senthil kumaar S., Varadarajan P.R., Porkodi K., Subbhuraam C.V. 2005. J. Colloid Interface Science. 284, 78–82.
Shahryari Z., Soltani Goharrizi A., Mehdi Azadi M. 2010. . I. J of water resources and environmental engineering. 2, 16-28.
Stephansen R.J., Sheldo J.B. 1996. Water Res. 30, 781-792.
Suteu D., Bilba D. 2005. Acta chem. Slov. 52, 73-79.
Vousdria E., Fytianos K., Bozani E. 2002. Global Nest: The Int. J. 4, 75-83.
Wang X.S., Zhoub Y., Jing Y., Sun C. 2008A. J. Hazard. Mater. 157, 374-385.
Weber T.W., Chackravorti R.K. 1974. Inst. Chem. Eng. J. 20, 228-238.
Zou W., Bai H., Gao S., Li K. 2013. J. Chem. Eng., 30 (1), 111-122.